

NOTICE CONCERNING COPYRIGHT RESTRICTIONS

This document may contain copyrighted materials. These materials have been made available for use in research, teaching, and private study, but may not be used for any commercial purpose. Users may not otherwise copy, reproduce, retransmit, distribute, publish, commercially exploit or otherwise transfer any material.

The copyright law of the United States (Title 17, United States Code) governs the making of photocopies or other reproductions of copyrighted material.

Under certain conditions specified in the law, libraries and archives are authorized to furnish a photocopy or other reproduction. One of these specific conditions is that the photocopy or reproduction is not to be "used for any purpose other than private study, scholarship, or research." If a user makes a request for, or later uses, a photocopy or reproduction for purposes in excess of "fair use," that user may be liable for copyright infringement.

This institution reserves the right to refuse to accept a copying order if, in its judgment, fulfillment of the order would involve violation of copyright law.

Geothermal Reservoir Characterization by Tracer and Well Testing

Serhat Akin¹ and Ender Okandan²

¹Stanford University Petroleum Research Institute and ²Petroleum Research Center
Middle East Technical University

ABSTRACT

This work presents the analysis of experimental data obtained on a lab scale fractured geothermal model where matrix block sizes, fracture apertures and distributions are known. The ultimate goal is to obtain the fracture aperture which is a key parameter in determining the flow and transport characteristics of fractured media. For the tracer tests, 4,000 ppm potassium iodide solution slug was injected from the corner of the model prepared using seventy stacked marble blocks and production concentration of the tracer was monitored from the other end of the diagonal. Drawdown pressure transient tests were conducted using the same model. Results indicated that flow was mainly through a major fracture path and tracer also entered to this path from auxiliary side fractures. The apparent size of the main fracture path was calculated as average 30 microns and secondary fractures had the average size of 10 microns which was found to be in good agreement with the mechanical aperture of 13.58 microns. The apparent fracture apertures, calculated using the permeability obtained from the well test analysis, changed from 70 microns to 116 microns overestimating the mechanical fracture aperture.

Introduction

Reservoir characterization includes all techniques and methods that improve understanding the geological and petrophysical properties that control the fluid flow. The objective is to provide practical reservoir models for optimum field development. Tracer study has become an important technique for reservoir characterization, particularly in such specialized areas as geothermal engineering, oil reservoir engineering (Baldwin, 1966), and hydrology (Rubbin and James, 1973).

Several processes generally act simultaneously on a chemical constituent while it is transported through a porous medium. Among these, the two primary processes are the physical phenomena of convection and hydrodynamic dispersion. While convection deals with the bulk movement of fluids, hydrodynamic dispersion describes the actions of molecular dispersion

and shear or mechanical mixing. These transport processes normally are represented adequately by the well known convection-dispersion diffusion equations with or without chemical reactions. Most of the time, these diffusion equations are based on linear or one dimensional geometry, largely because of the relative ease with which such equations can be solved analytically.

Interpretation of tracer tests involve matching tracer data from the field by use of computer simulation programs utilizing aforementioned models. As the complexity of the simulator model increases, the number of trial runs needed to fit field data satisfactorily increases rapidly. The conventional fitting procedure can thus become very cumbersome and can involve prohibitive computer costs. In this study, a methodology proposed by Akin and Okandan (1995) was used to model tests conducted in fractured geothermal models. In this methodology, rigorous simulators have been replaced by simple response functions generated in a spreadsheet software. Therefore, matching the tracer data involves function evaluations rather than full simulator runs, resulting in a large reduction in computing time.

In petroleum engineering and groundwater hydrology, well tests are conducted routinely to diagnose the well's condition and to estimate formation properties. Well test data may be analyzed to yield quantitative information regarding (1) formation permeability, storativity, and porosity, (2) the presence of barriers and leaky boundaries, (3) the condition of the well (i.e., damaged or stimulated), (4) the presence of major fractures close to the well, and (5) the mean formation pressure. A major concern of well testing is the interpretation of pressure transient data. Pressure transient technique is, perhaps, the most used method to obtain basic reservoir parameters other than tracer testing. Since geothermal wells usually produce from fractured volcanic rocks and due to the fact that naturally fractured reservoirs exhibit a production behavior quite different from that of conventional homogeneous reservoir, it is particularly important to try to establish the dimensions of the fractured system. An estimation of the fractured system parameters such as fracture pore

volume, directional trends, storage capacity, etc. is highly valuable for the purpose of selecting development drilling locations and planning of exploitation strategies.

Theory

Tracer Tests

The flow of tracer between an injection and a production well pair has been described both analytically and numerically by a number of authors. The governing equation modeling the flow of a tracer is the well known convection-dispersion diffusion equation which can be written in one dimensional form as follows:

$$\frac{\partial C}{\partial t} = -\eta \frac{\partial C}{\partial x} + D_L \frac{\partial^2 C}{\partial x^2} \quad (1)$$

In this study, the multi-fracture model proposed by Fossum and Horne (1982) was used to solve this equation. This model, assumes a single or multi-fracture system, joining the injection and observation wells. Dispersion is due to the high velocity profile across the fracture and molecular diffusion, which moves tracer particles between streamlines (Taylor dispersion). The transfer function C_t is given by the following expression:

$$C_t = \sum_{i=1}^n e_i C_r(L_i / u_i, P_{ei}) \quad (2)$$

where n is number of flow channels in the fracture system, e_i is the flow contribution coefficient, L_i is the apparent fracture length, u_i is the velocity, and P_{ei} is the Peclet number of the i^{th} flow channel. Therefore if "n" is taken as one then only a single fracture is present. It should be noted that for all practical purposes, a multi fracture system must be represented with at least two fractures, since it has been reported by Akin and Okandan (1995) that the value of the transfer function, C_t does not change much as n increases. The form of C_r for each of the paths for a mass of tracer concentrated at point $x=0$ at time=0 is:

$$C_r = \frac{1}{2\sqrt{\frac{t_r}{P_e}}} \text{Exp} \left[-\frac{(1-t_r)^2}{\frac{4}{P_e} t_r} \right] \quad (3)$$

where P_e is the dimensionless Peclet number and t_r is the mean arrival time. Using the above model, by knowing the coefficient of molecular diffusion, D , it is possible to obtain the average velocity, length, mean arrival time, and inferred fracture aperture, b for each flow channel by using the following definition for dispersivity, η (Rodriguez and Horne, 1983):

$$\eta = \frac{2b^2u^2}{105D} \quad (4)$$

Pressure Transient Tests

During a well-test, the response of a reservoir to changing production or injection conditions is monitored. Since the response is characteristic of the properties of the reservoir, it is possible to gather reservoir properties from the response. The aim of well-test interpretation is therefore, to obtain one or more of the following parameters and functions (Da Prat, 1990):

1. Average permeability.
2. Initial or average reservoir pressure.
3. Sand-face condition (damage or stimulation).
4. Volume of the drainage area.
5. Degree of communication between wells.
6. Validation of the geological model.
7. System identification.

Geothermal wells generally produce from fractured volcanic rocks. As reported by Barenblatt et al (1960), a porous rock with a highly developed system of fissures can be represented as the superposition of two porous media with pores of different sizes. Warren and Root (1963) presented a model based on above mathematical concept of superposition. They idealized a naturally fractured reservoir such that the material with the primary porosity is contained within a systematic array of identical rectangular parallelepipeds. The secondary porosity is contained within an orthogonal system of continuous uniform fractures which are oriented parallel to one of the principal axes of permeability. In this model, the dual porosity effects are described in terms of two parameters that relate primary and secondary properties. The first of the two parameters is the storativity ratio, ω , that relates the fracture storativity to that of the combined flow:

$$\omega = \frac{\phi_f C_{ff}}{\phi_f C_{ff} + \phi_m C_{fm}} \quad (5)$$

Values of ω can be less than or equal to one. The case of $\omega = 1$ occurs if the matrix porosity is zero, hence it implies that the reservoir is a single porosity one (Horne 1995).

The second parameter is dependent on the transmissivity ratio, and is designated as λ :

$$\lambda = \alpha \frac{k_m r_w^2}{k_f} \quad (6)$$

Here α is a factor that depends on the geometry of the interporosity flow between the matrix and the fractures:

$$\alpha = \frac{A}{xV} \quad (7)$$

where A is the surface area of the matrix block, V is the matrix volume, and x is a characteristic length. If the matrix blocks are cubes or spheres, then the interporosity flow is three dimensional and λ is given by

$$\lambda = \frac{60k_m r_w^2}{x_m^2 k_f} \quad (8)$$

where x_m is the length of a side of the cubic block, or the diameter of the spherical block. If the matrix blocks are long cylinders, then the interporosity flow is two dimensional and λ is given by

$$\lambda = \frac{32k_m r_w^2}{x_m^2 k_f} \quad (9)$$

where x_m is now the diameter of the cylindrical block. If the matrix blocks are slabs overlying each other with fractures in between, then the interporosity flow is one dimensional, and λ is given by

$$\lambda = \frac{12k_m r_w^2}{h_f^2 k_f} \quad (10)$$

where h_f is the height of the secondary porosity slab.

Values of λ are usually very small (usually, 10^{-3} to 10^{-10}). If the value of λ is larger than 10^{-3} , the level of heterogeneity is insufficient for dual porosity effects to be of importance, and again the reservoir acts as a single porosity (Horne 1995) as in the case of $\omega = 1$.

Analysis of pressure transient tests are usually conducted by combining type-curve matching and semi-logarithmic techniques in a computer aided manner.

Description of Laboratory Tests

The experimental laboratory tests studied in this work were conducted and reported in detail by Bayar (1987). In the experimental work, tracer flow and pressure drawdown in a fractured geothermal model with zero matrix permeability was considered.

A three dimensional model composed of 70 pieces of marble blocks in three different sizes as shown in Figure 1 was built. Marble blocks with dimensions 10x10x10cm, 10x10x20cm, and 5x10x20cm were placed freely on top of each other. A box frame of 60x60x60 was used to cover the fractured medium created and porosity of the medium was determined as 4% that indicated 5850 cc pore volume. Potassium Iodide (KI) solution was used as the chemical tracer and it was injected from the diagonal corner of the model and production concentration of the tracer was monitored from the other end of the diagonal. Injection and production depth was changed to observe the effect of longer path of travel in the fractures. Volume of KI slug injected was one third of the pore volume with the concentration of 4000 ppm for each run. The experimental runs were named from B1 to B4 and the injection-production scheme was as follows: B1, top-bottom; B2, bottom-top; B3, top-top; B4, bottom-bottom. A total of four tracer tests and eight drawdown tests were analyzed.

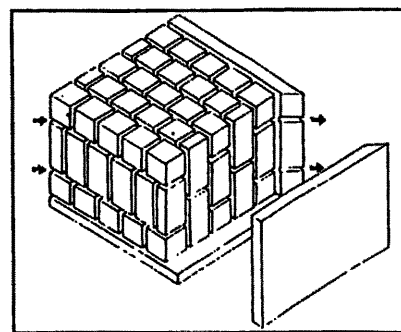


Figure 1. Schematic diagram of the experimental set-up (Bayar 1987).

Method of Solution

Tracer Tests

The developed analytical model was implemented on a commercially available spreadsheet software (Microsoft Excel) for convenience as reported by Akin and Okandan (1995). The model was then matched to experimental data using least squares approximation with a combination of a well-known nonlinear optimization code namely GRG2 (Lasdon and Waren, 1989) which is also utilized in the spreadsheet software (Microsoft Excel User's Guide, 1992). By minimizing the following objective function R ,

$$R = \sum_{i=1}^n (C_r - C_{exp})^2 \quad (11)$$

the parameters of the proposed analytical transfer function C_r can be estimated. In nonlinear parameter estimation or curve fitting, it is important to have good initial estimates for the model parameters. The peak time and response start time can be easily found from the test data. However, initial estimates for the nonlinear parameters (i.e. Peclet number) should be carried out in trial and error fashion. The methodology can be summarized as follows. First the problem is defined by specifying the target cell (R), changing cells (Pe , etc.), and the constraints ($Pe > 0$, etc.). Following that the solution process is controlled by defining the solution time, number of iterations, and the precision of constraints. Then the method used by the "Solver" is defined. At this point, the estimation technique (tangent or quadratic), the method for calculating derivatives (central difference equation or forward difference equation), and finally the search method (quasi-Newton or conjugate) must be defined.

After the "Solver" has found a solution, to specify the goodness of the estimate, confidence intervals of the changing parameters were found. Using 95 % confidence intervals to evaluate the goodness of fit of a nonlinear regression analysis of tests, it was observed that an acceptable estimate was the one with a confidence interval that is 10% of the value itself. If the confidence interval of one of the changing parameters exceeds the aforementioned value, initial estimates of the changing parameters were readjusted and/or the search direction and the esti-

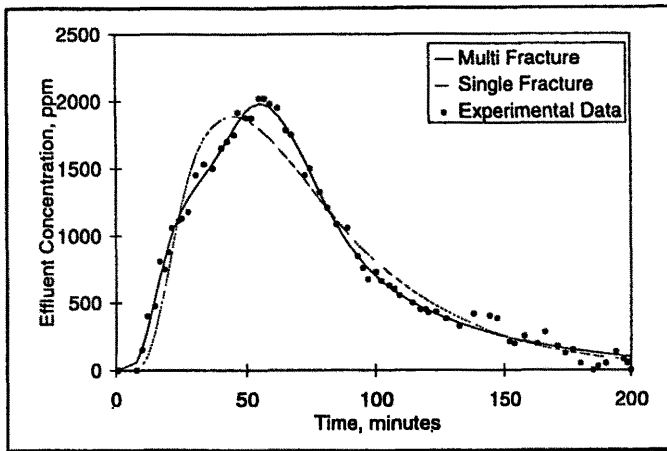


Figure 2. Matches to the Response of Experiment B1.

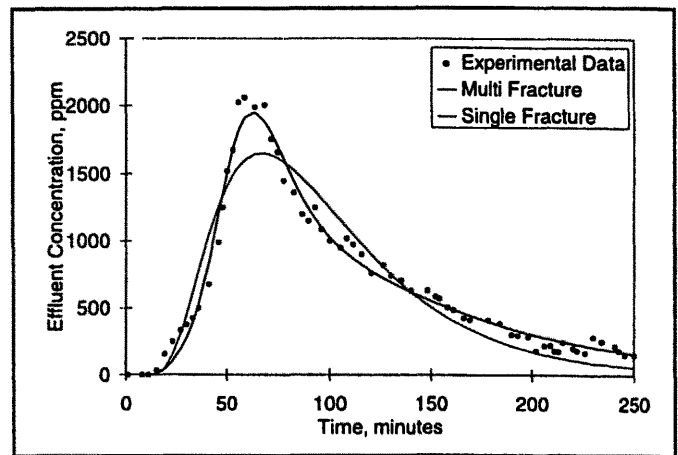


Figure 5. Matches to the Response of Experiment B4.

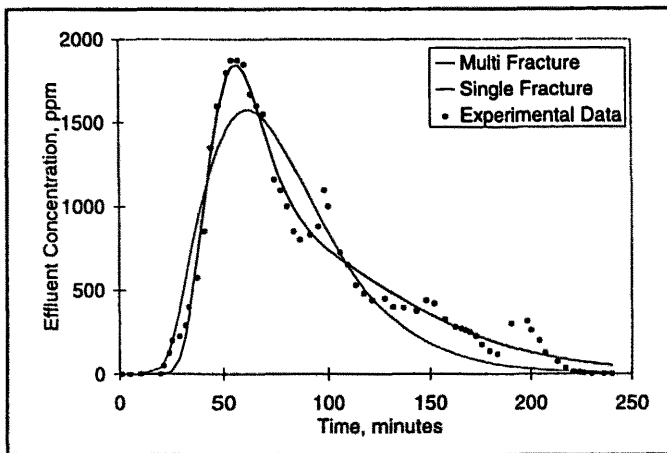


Figure 3. Matches to the Response of Experiment B2.

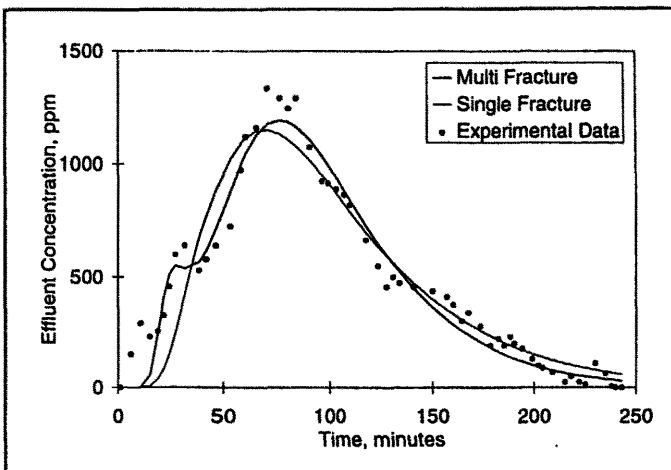


Figure 4. Matches to the Response of Experiment B3.

mates were changed until a reasonable value was achieved. It should be noted that, the confidence interval is a function of noise in the data, as well as the number of data points, and the degree of correlation between the unknowns.

Drawdown Tests

Analysis of pressure transient tests were carried out in a systematic manner similar to that of tracer test analyses. The first step consisted of conventional semilog and type curve analysis (Horne 1995). Initial parameter estimates for several reservoir parameters like permeability were obtained at this stage. Then these estimates were fine tuned using an automated history matching technique. The estimated parameters were accepted using aforementioned 10% confidence intervals. The analyses were conducted using a commercial well test analysis package named Automate™ (Horne 1995). During the estimation procedure three types of wellbore conditions were considered: wellbore storage and skin, finite conductivity vertical fracture, and infinite conductivity vertical fracture.

Results and Discussions

Tracer Tests

The analysis results for the multi-fracture model are summarized in Table 1 and represented schematically in Figures 2 through 5. As it can be seen from the results that, there are secondary fractures yielding high fluid velocity and small mean arrival time. The equivalent aperture of this fracture system is between 9.65 and 13.24 microns. These findings were in very good agreement with the mechanical fracture aperture (Reiss 1980) which was calculated to be 13.58. It has been also observed that the mean arrival times obtained are in good agreement with the experimental data as it can be observed from the matches to the twin peaked response curves. For this model, the dimensionless parameter ϵ , which can be regarded as a weighing factor, the contribution of the main (first) fracture is more than the secondary fractures. The dispersion coefficients in the first fracture system was lower than the secondary fractures,

which shows that the loss of tracer to the secondary fractures was more.

For the secondary flow path Peclet numbers are larger when compared to the shorter main fracture path meaning a convection dominant system. However, for the main flow path the fluid velocity and the fracture length is relatively small and yields smaller Peclet numbers. It should be noted that the apparent fracture aperture is larger (about 30 microns) when compared to the secondary flow path.

However, if we assume our fractured reservoir can be modeled by a single fracture, there is a distinct difference between the effective dispersion coefficients obtained from the multi-fracture model (Table 2). Dispersion coefficients were ten times greater than the multi-fracture dispersion coefficients which is an indication of insignificant molecular diffusion. However, mean arrival times and the fracture apertures were in agreement apart from slight differences with the main fracture system observed in the previous model. Moreover, since the fracture aperture estimates were larger compared to the mechanical aperture, it can be concluded that a single fracture model can not describe the flow process.

Table 1. Results of Multi Fracture Model

First Fracture							
	P_e	e	u	L	t_m	h	b
	dmls	dmls	cm/min	cm	min	cm ² /min	μm
B1	3.48	1.21	0.71	36.47	51.29	7.64	35.93
B2	10.03	0.39	0.37	36.47	97.60	1.36	29.17
B3	9.96	0.65	0.13	11.03	83.71	0.15	27.11
B4	4.90	0.73	0.39	36.47	94.32	2.88	41.04

Second Fracture							
	P_e	e	u	L	t_m	h	b
	dmls	dmls	cm/min	cm	min	cm ² /min	μm
B1	30.49	0.25	2.11	128.95	61.08	8.93	13.24
B2	34.69	0.43	2.33	128.95	55.36	8.66	11.82
B3	25.87	0.17	6.47	178.08	27.52	44.55	9.65
B4	32.38	0.33	2.04	128.96	63.15	8.13	13.07

Table 2. Results of Single Fracture Model

	P_e	e	u	L	t_m	h	b
	dmls	dmls	cm/min	cm	min	cm ² /min	μm
B1	5.31	1.38	6.21	339.50	54.68	397.29	30.03
B2	10.38	0.85	5.03	339.52	67.48	164.65	23.86
B3	6.79	0.76	4.26	339.54	79.67	213.01	32.04
B4	7.14	1.06	4.40	339.53	77.23	208.96	30.76

Drawdown Tests

A total of eight drawdown tests which correspond to four different injection and production scheme were analyzed. Four some of the tests, it has been observed that the characteristic "S" shape of naturally fractured reservoirs that is seen in a semilog

plot of pressure versus time was not present. Figure 6 gives an example of a fully developed "S" shaped and an incomplete semilog plot of two drawdown tests. For such incomplete tests, the "V" shaped characteristic derivative plot attributed to the naturally fractured reservoirs was not observed either.

The models and their different combinations presented in Table 3 were used to match experimental drawdown data. It has been observed that, for most cases since the boundary effects were not visible the use of "Closed Circle" and "Closed Rectangle" boundary conditions was not necessary. Hence, "Infinite Acting" boundary condition was used for the analyses. Similarly, both transient and pseudo steady state double porosity model results were close to each other leaving only three possible and equally probable models: 1) storage-skin homogeneous model, 2) finite conductivity fracture wellbore with transient double porosity model and 3) storage-skin homogeneous infinite acting model.

Table 3. Well Test Models Used for Matching Data.

Model	1	2	3
Wellbore	Storage Skin	Finite Conductivity Fracture	Storage Skin
Reservoir	Homogeneous	Dual Porosity Transient	Dual Porosity PSS
Boundary	Infinite Acting	Closed Circle	Closed Rectangle

Model 1

This type of model is one of the most generally used well test models to represent geothermal reservoir conditions since, large wellbore storage coefficient is common in geothermal wells due to the large wellbore volume and the compressibility of the steam-water mixture in the wellbore. Table 4 presents the results of the analyses obtained using this model. Large, negative skin values calculated are consistent with the theory that since geothermal wells generally produce from fractured volcanic rocks they show stimulated behavior (Horne 1995). However, fracture width values calculated from the permeability data (Reiss 1980) overestimated the mechanical fracture aperture many times.

Table 4. Results Obtained from Homogeneous - Storage - Skin Model.

Test #	Port	k, md	$b, \mu\text{m}$	Skin	Cde2S
28	TB	21.36	98.09	-8.17	8.670e0
30	TB	57.12	160.40	-6.99	2.748e1
31	BT	117.31	229.87	-1.88	2.721e5
27	BT	87.33	198.34	-0.89	1.443e7
34	TT	61.29	166.16	-3.27	1.718e4
36	TT	98.32	210.45	-3.77	8.289e3
37	BB	75.34	184.22	-3.47	9.949e3
41	BB	19.59	93.94	-7.68	2.762e3

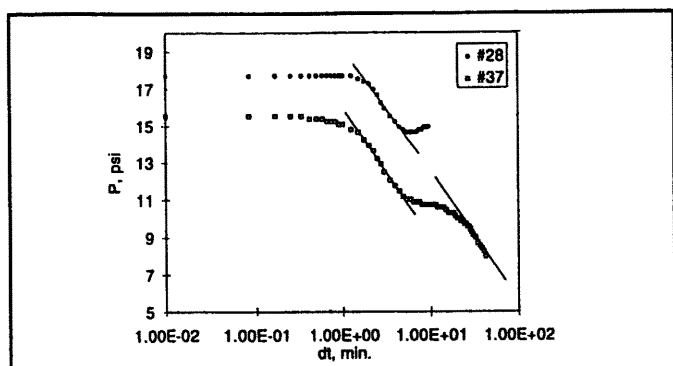


Figure 6. Semilog plot showing complete and incomplete drawdown tests.

Finite conductivity fracture - double porosity pseudo steady state model was one of the closest model to the physics and the nature of the experiments. Although, the magnitude of sum of squares residuals obtained from this model were slightly better when compared to the previous model, the fracture aperture estimates were not extremely better. The values of lambda and omega were found to be consistent with zero matrix permeability of the marble blocks.

Table 5. Results Obtained from Finite Conductivity - Dual Porosity Transient Model.

Test #	Port	k, md	b, μm	Xf, cm.	ω	λ
28	TB	52.1	153.2	17.9	2.5e-7	3.7e-4
30	TB	28.7	113.7	12.9	2.1e-6	7.1e-2
31	BT	53.3	154.9	19.7	1.3e-5	1.1e-2
27	BT	38.9	132.4	11.7	9.8e-5	7.8e-6
34	TT	20.3	95.6	33.8	2.1e-7	1.1e-3
36	TT	29.7	115.7	20.5	1.2e-6	5.5e-2
37	BB	22.8	101.34	19.5	1.2e-7	6.2e-4
41	BB	25.1	106.3	17.4	4.7e-7	3.2e-3

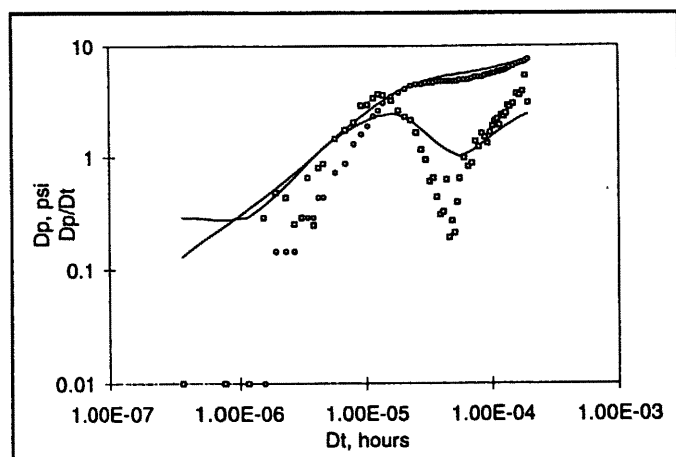


Figure 7. Storage-Skin Dual Porosity PSS Model Match to Data from Experiment 37.

Model 3

The final model considered was storage-skin double porosity transient model. The sum of squares residuals obtained from this model were comparable to the second model. Moreover, the fracture apertures were much more better than the previous models and the lambda values were consistent with zero matrix permeability of the physical model. However, the omega values were many times larger, suggesting an almost homogeneous system. An interesting observation was that the storage values were somewhat small which is not common in geothermal well tests. Figure 7 gives one of the experimental fits obtained using this model. It can be observed that early time region was not modeled adequately with the storage-skin model. An interesting observation that was common to all models that the log-log slope values were greater than unity for all tests.

Table 6. Results Obtained from Storage - Skin - Dual Porosity Transient Model.

Test #	Port	k, md	b, μm	Skin.	ω	λ	Cde2S
28	TB	15.0	82.20	-0.26	0.54	1.9e-9	3.26
30	TB	30.2	116.63	-0.73	0.34	1.2e-2	1.15
31	BT	16.5	86.21	-0.067	0.18	8.0e-9	16.2
27	BT	11.7	72.60	-0.28	0.23	7.7e-9	15.0
34	TT	11.3	71.34	-0.09	0.43	5.1e-8	3.24
36	TT	20.0	94.92	-0.52	0.29	3.1e-9	3.39
37	BB	13.2	77.11	-0.33	0.30	9.e-11	2.47
41	BB	16.7	86.73	-0.21	0.33	1.7e-5	2.06

Another interesting observation was that although the same physical model was used in all experiments, the injection-production scheme change resulted in close but different parameter values (i.e. permeability, fracture aperture, etc.). This observation was valid for all models. Fractal geometry may be a solution to this phenomenon as suggested by Acuna et al. (1995).

Conclusions

Tracer and drawdown tests conducted on a fractured laboratory model with zero matrix permeability were analyzed and reported. Based on the matching results the following conclusions can be done.

1. Tracer results indicated that flow was mainly through a major fracture path and tracer also entered to this path from auxiliary side fractures. The apparent size of the main fracture path was calculated as average 30 microns and secondary fractures had the average size of 10 microns which was found to be in good agreement with the mechanical aperture of 13.58 microns.
2. Drawdown well tests can be described with storage-skin dual porosity models as well as finite conductivity fracture dual

porosity models. Homogeneous models with negative skins can not describe the process better than the other models.

3. The average fracture aperture calculated from the permeability data obtained from drawdown tests overestimated the mechanical aperture.
4. Finally, although all tests were conducted using the same model, the injection-production scheme change resulted in similar but different responses encouraging the use of fractal well test models.

Nomenclature

A = area
 b = fracture aperture
 C = concentration
 C_{exp} = experimental concentration
 C_r = observed concentration
 C_{fr} = fracture compressibility
 C_{m} = matrix compressibility
 D = dispersion coefficient
 e = flow coefficient
 hf = height
 k_f = fracture permeability
 k_m = matrix permeability
 n = number of flow channels
 P_e = Peclet number
 r_w = wellbore radius
 t = time
 t_r = mean arrival time
 u = velocity
 V = volume
 x = spatial variable
 x_f, L = fracture length
 X_m = length
 λ = transmissivity ratio
 h = effective dispersion coefficient
 ϕ_f = fracture porosity

ϕ_m = matrix porosity

ω = storativity ratio

References

- Acuna, J.A., Ershaghi, I. and Yortsos, Y.C., 1992. "Practical Application of Fractal Pressure-Transient Analysis in Naturally Fractured Reservoirs," paper SPE 24705 presented at the SPE Annual Technical Conference and Exhibition held in Washington, D.C. October 4-7.
- Akin, S. and Okandan, E., 1995. "Reservoir Characterization by Tracer Testing," presented at the World Geothermal Congress 1995, 18-31 May, Florence, Italy.
- Baldwin, D. E. Jr., 1966. "Prediction of Tracer Performance in a Five-Spot Pattern," JPT, April 513-17.
- Barrenblatt, G.I., Zheltov, I.P. and Kochina, I.N., 1960. "Basic Concepts in the Theory of Homogeneous Liquids in Fissured Rocks," *J. Appl. Math. Mech.*, no. 24, p. 1286-1303.
- Bayar, M. 1987. "Tracer Testing in a Fractured Geothermal Reservoir Model," Msc Thesis, METU, Ankara, Turkey.
- Da Prat, G., 1990. "Well Test Analysis for Fractured Reservoir Evaluation," Elsevier, Science Publishing Company Inc., New York, U.S.A.
- Fossum, M.P. and Horne, R.N., 1982. "Interpretation of Tracer Return Profiles at Wairakei Geothermal Field Using Fracture Analysis," *Geothermal Resources Council Transactions*, vol. 6, p. 261-264.
- Horne, R. N., 1995. "Modern Well Test Analysis-A Computer Aided Approach," Petroway Inc., Palo Alto, CA, U.S.A.
- Lasdon, L. and Waren, A., 1989. GRG2 User's Guide.
- Microsoft Excel User's Guide, 1992. Microsoft Corporation, One Microsoft Way, Redmond.
- Reiss, H.L., 1980. "The Reservoir Engineering Aspects of Fractured Formations," Gulf Publishing Company, Houston, Texas.
- Rodriguez, and Horne, R.N., 1983. *Geophysical Research Letters*, no. 10, p. 289-290.
- Rubbin, J. and James, R.V., 1973. "Dispersion Affected Transport of Reacting Solute in Saturated Porous Media: Galerkin Method Applied to Equilibrium Controlled Exchange in Unidirectional Steady Water Flow," *Water Resources Res.*, no. 5, p. 1335-56.
- Warren, J.E. and Root, P.J., 1963. "The Behavior of Naturally Fractured Reservoirs," *SPE Journal*, September, p. 245-255.